Study of physical and magnetic properties of Mg:Co_3O_4 spinels using L-Arginine as fuel

M. Sundararajan[a,], J. Vidhya[b], R. Revathi[c], M. Sukumar[d], V. Ravi[e], R. Rajkumar[f], M. Kamalakannan[g], C. S. Dash[h,], H. Lohedan[i,] R. Jothi Ramalingam[*i], S. Arokiyaraj[j]

[a]*PG & Research Department of Physics, Paavendhar College of Arts & Science, M.V. South, Attur, Salem, Tamilnadu 636 121, India*

[b]*Department of Physics, M Kumarasamy College of Engineering, Karur, Tamil Nadu 639 113, India*

[c]*Department of Biotechnology, Periyar University PG Extension Centre,Dharmapuri, Tamil Nadu 636 701, India*

[d]*Department of Physics, Anand Institute of Higher Technology, Kazhipattur, Chennai, 603103, India*

[e]*School of Electronics Engineering, VIT University Chennai Campus, Chennai-600 127,Tamilnadu, India.*

[f]*Department of Electronics and Communication Engineering, Vel Tech Rangarajan Dr Sagunthala R&D Institude of Science and Technology, Chennai, Tamilnadu600 062, India*

[g]*Department of Basic Sciences, College of Fisheries Engineering, Dr. J. Jayalalithaa Fisheries University, Nagapattinam-611 002, India*

[h]*Department of Electronics and Communication Engineering, Centurion University of Technology and Management, Odisha, Bhubaneswar-752 050, India*

[I]*Department of chemistry, College of Science, King Saud University, P.O. Box. 2455, Riyadh 11451, Saudi Arabia.*

[j]*Department of Food Science and Biotechnology, Sejong University, South Korea*

Magnesium doped cobalt oxide nanoparticles were synthesized via microwave assisted combustion method (MACM). The X-ray diffraction (XRD) patterns of pure Co_3O_4 and Mg^{2+} doped Co_3O_4(x = 0.1 and 0.3) confirmed the cubic spinel structure and without any additional impurity peaks. However, doping Mg^{2+} concentration, x = 0.3 and 0.5 sample was occur a new hexagonal phase, while the average crystallite size of the cubic spinel structure in the range from 48.5 nm to 15.5 nm. The FT-IR bands at 661 and 573 $cm^{-1}$are attributed to the Co–Ostretching mode of cubic spinel Co_3O_4 structure. The band gap calculated using Kubelka–Munk (K–M) technique and increasedband gap values withthe increase in Mg^{2+} content (1.87–3.60 eV), due to the causes of sub-bands in the energy band gap. The morphological study revealed the prepared samples exhibited intragranular pores and merged grains with discrete grain boundaries.Magnetization analysis revealed the appearance of para-/superpara- magnetic behavior at ±15KOe.

(Received June 25, 2021; Accepted October 11, 2021)

Keywords: $Co_{1-x}Mg_xO_4$ nanoparticles, Optical analysis, Structural analysis, Vibrational analysis, Magnetic analysis

1. Introduction

Currently due to their structural, electrical, thermal and magnetic properties porous type materials started gaining so much of attention. They are employed in distinct technological applications like batteries, solid-state sensors, heterogenous catalyst, energy storage, solar energy absorbers, gas sensors and super capacitors [1-3]. It is also used in

* Corresponding author: jrajabathar@ksu.edu.sa

electrochemical devices due to its high surface area and volume [4,5]. Cobalt oxide is usually used as magnetic materials because they show notable photo-electrochemical properties. Owing to its excellent stability it shows electro catalysis and also posses other promising abilities. Co_3O_4 and Co- based nanocomposite materials are utilized as an enhancement agent for magnetic resonance imaging and medical applications [6-8]. Cobalt oxide is a transition metal oxide having cubic normal spinel crystal structure. Importantly it is an attractive p-type semiconductor material emitting anti ferromagnetic behavior with Neel temperature (T_N) of ~30 K [9, 10]. There exist two positive pathways due to super exchange interactions for CoO_3 possessing anti ferromagnetic behavior and they are (i) $Co^{2+} - O - Co^{3+} - O - Co^{2+}$, (ii) $Co^{2+} - O - Co^{2+}$. Fundamentally Co_3O_4 possesses a narrow band gap (~0.74 eV) due to direct dipole forbidden d-d transition between tetrahedral site Co^{2+} cation [10, 11]. Rock salt structure of Cobalt (II) oxide (CoO) or spinel cobalt (II, III) oxide with mixed oxidation state (Co^{2+} and Co^{3+}) are the common structures in which Co_2O_3 and Co_2O_4 compounds will exist. Generally during the crystallization of Co_3O_4, the non-magnetic Co^{3+} ions occupy the octahedral sites whereas the magnetic Co^{2+} ions occupy the tetrahedral sites. As we all know that oxides are abundant in nature, among them CoO and Co_3O_4 are stable oxides further Co_3O_4 possesses the highest stability [10, 14].

Since reports on the preparation of MgO and Co_3O_4 using microwave combustion method is very rare, in this paper we have synthesized Mg^{2+} doped Co_3O_4 nanoparticles utilizing the microwave combustion method. A secondary phase (MgO at x = 0.3 and 0.5) is examined because of the effect of Mg^{2+} on Co_3O_4 under the influence of microwave. Owing to thermo chemical stability, good conductivity and low production cost $Mg^{2+}$is doped with Co_3O_4 nanoparticles. In this present study, Mg^{2+} doped Co_3O_4 nanoparticles are synthesized using MACM method. The produced samples are physically characterized to study its thermal, optical, magnetic characteristics and surface morphology. The observed results are elaborately discussed in the succeeding sections as follows.

2. Experimental

2.1. Materials

Magnesium nitrate (Mg $(NO_3)_2.6H_2O$), Cobalt nitrate (Co $(NO_3)_2$. $4H_2O$) and L-alanine of analytical grade are bought from SD fine- chemicals, India. The purchased chemicals were directly used without any further purification. Double distilled water was utilized for preparing the samples.

2.2. Synthesis of Mg^{2+} doped Co_3O_4 nanoparticles

The spinel nanoparticles were synthesized using Cobalt nitrate (oxidizers), magnesium nitrate (oxidizers) and L- arginine as fuel through MACM. The fuel-to-oxidizers (F/O) ratio was maintained to be 1 on the basis of the principle of propellant chemistry. The obtained sample solution of homogenous condition was further mixed with de-ionized water and stirred for about 1h at 300K. The homogenous solution was heated in microwave oven (750 W) at a frequency of 2.45GHz for about 15 minutes,

The heated homogenous solution on reaching the threshold temperature undergoes dehydration first and then lastly it decomposes. A black fluffy powdery substance was finally obtained. The obtained sample was further washed with ethanol followed by calcination at 550 ^oC for 120min. The prepared samples are labelled as x= 0.0, x= 0.1, x= 0.3 and x= 0.5, it was characterized using XRD, HR-SEM, EDX, DR-SUV, FTIR, and VSM respectively.

3. Results and discussion

3.1. X-ray diffraction analysis

The obtained samples XRD patterns are shown in Figure 1. The peaks of pure Co_3O_4 and $Mg_{0.1}Co_{0.9}O_4$ matches well with the JCPDS card No: 1003, exhibiting single phase and cubic structure with space group $Fd\bar{3}m$. The characteristics peaks observed at 19.11°, 31.24°, 36.85°, 38.45°, 44.77°, 59.23°, 65.22° are indexed as the (111), (220), (311), (222), (400), (511), and (440) crystallographic planes correspondingly. Additionally at sample concentration $Mg_{0.3}Co_{0.7}O_4$ and $Mg_{0.5}Co_{0.5}O_4$ extra peaks are noted and it matches with the JCPDS card no 89-7746 [14]. On increasing the Mg^{2+} concentration x =0.3 and 0.5 a new secondary MgO phase (space group *P63mc*) with hexagonal structure with peaks at $2\theta \approx 42.55°$ (100), 61.89° (002) [15]. A two-phase system with cubic (Co_3O_4) and hexagonal (MgO) was formed due to the substitution of Co^{2+} by Mg^{2+} ions resulting in the composite formation. On increasing the Mg^{2+} concentrations, the intensity of the peak referring to hexagonal phase decreases.

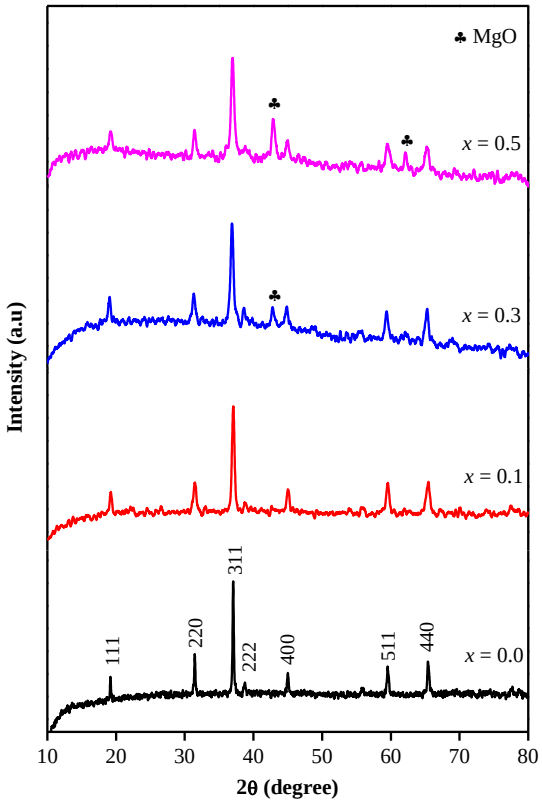

Fig. 1. X-ray diffraction patterns of the Mg^{2+} doped Co_3O_4 nanoparticles.

3.2. Optical properties

Figure 2 represents the energy gap values of pure and Mg doped cobalt oxide nanoparticles. Equation 1 gives the modified Tauc relation [20] which is used to deduce the optical energy band gap as follows,

$$F(R) = A\,(h\nu - E_g)^n \qquad (1)$$

The values of Mg^{2+} doped Co_3O_4 NPs are estimated to be about 1.87, 3.60, 3.52 and 3.40eV for x = 0, 0.1, 0.3 and 0.5 respectively as given in Table 1. Between 1.87- 3.60 eV for x = 0 and 0.1 there is an increase in band gap observed due to doping of Mg^{2+}. Owing to the creation of sub bands, variation of band is noted between the energy band gap. Continuous bands resulting in lowering

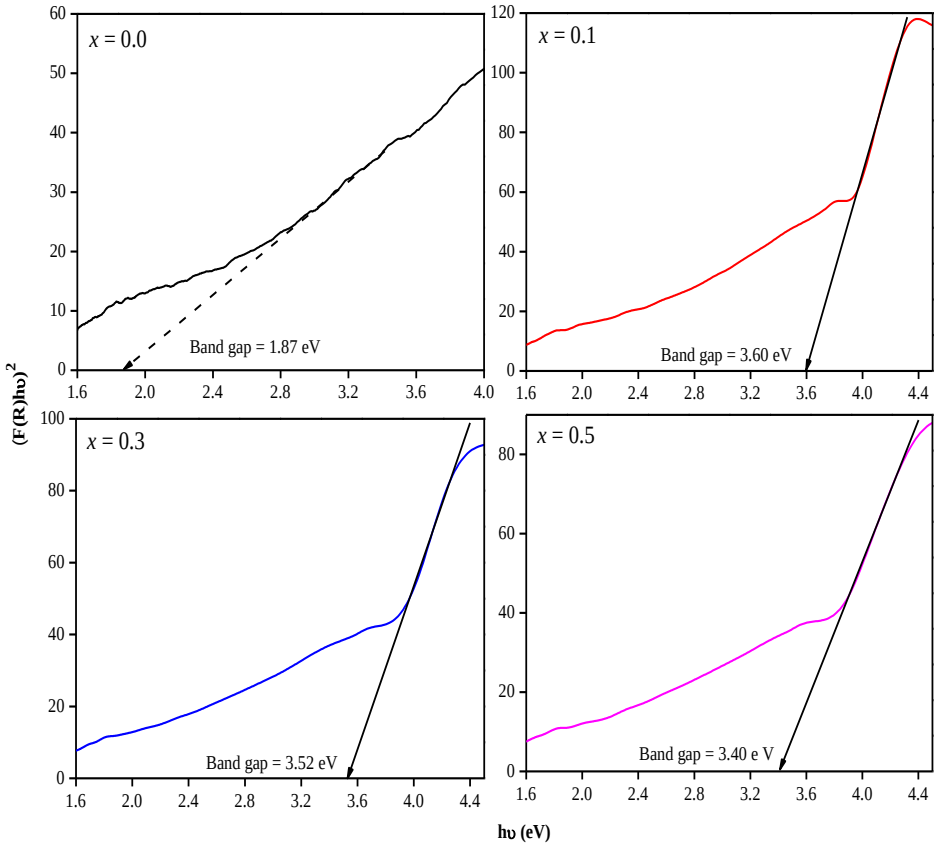

Fig. 2. Plot of $(F(R)hv)^2$ versus hv (eV) for the Mg^{2+} doped Co_3O_4 nanoparticles.

Table 1. Crystallite size, lattice parameter, cell volume and energy gap of Mg^{2+} doped Co_3O_4 nanoparticles.

Sample Code	**Sample Name**	**Crystallite size *D* (nm)**	**Lattice Parameter,*a* (Å)**	**Cell volume ($Å^3$)**	**Bandgap (eV)**
x = 0.0	Co_3O_4	45.8	8.0613	523.86	1.87
x = 0.1	$Mg_{0.1}Co_{0.9}O_4$	21.0	8.0584	523.29	3.60
x = 0.3	$Mg_{0.3}Co_{0.7}O_4$	17.6	8.0242	516.66	3.52
x = 0.5	$Mg_{0.5}Co_{0.5}O_4$	15.5	8.0204	515.92	3.40

3.3. FTIR analysis

Figure 3 illustrates the Mg^{2+} doped Co_3O_4 NPs obtained by varying the wavenumber in the range of 4000 – 400cm^{-1}. The broad band at 3440 cm^{-1} corresponds to the O-H stretching vibration of the adsorbed H_2O molecules [17, 18]. The band at 2910 cm^{-1} is associated with asymmetric and stretching vibrations of C-H bonds. Further the band at 1624 cm^{-1} is due to H-O-H bond vibration. A weak band at 1380 cm^{-1} is due to the presence of residual nitrogen groups that occurred during the combustion technique. Another weal band at 1040 cm^{-1} is because of symmetric stretching of Co_3^{2-} ion. The bands at 661 and 573cm^{-1} are due to the fingerprint stretching vibrational modes of Co-O bonds, which further confirms the cubic Co_3O_4 NPs formation [16, 14]. A band at 474 cm^{-1} occurred due to the stretching vibration mode of hexagonal Mg-O bond through increased Mg^{2+} doping at x = 0.3 and 0.5, it further proves the high crystallinity of the sample which was confirmed from XRD (x = 0.3 and 0.5) analysis.

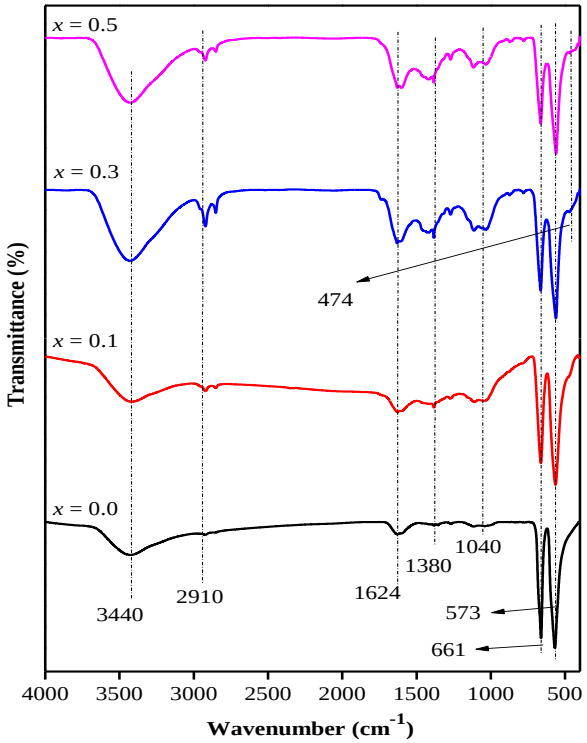

Fig. 3. FT-IR spectra of the Mg^{2+} doped Co_3O_4 nanoparticles.

3.4 SEM and EDX analyses

Figure 5 reveals the HRSEM images of the prepared samples. It confirmed the formation of porous and spherical nanosized crystallized grains because of the loss of water molecules and discharge of volatile gases during combustion. Energy dispersive X-Ray analysis is shown in Figure 6. Thus, the elemental composition of the Mg^{2+} doped Co_3O_4 NPs has been confirmed. i.e., The basic elements such as Co, Mg and O which was expected has been confirmed.

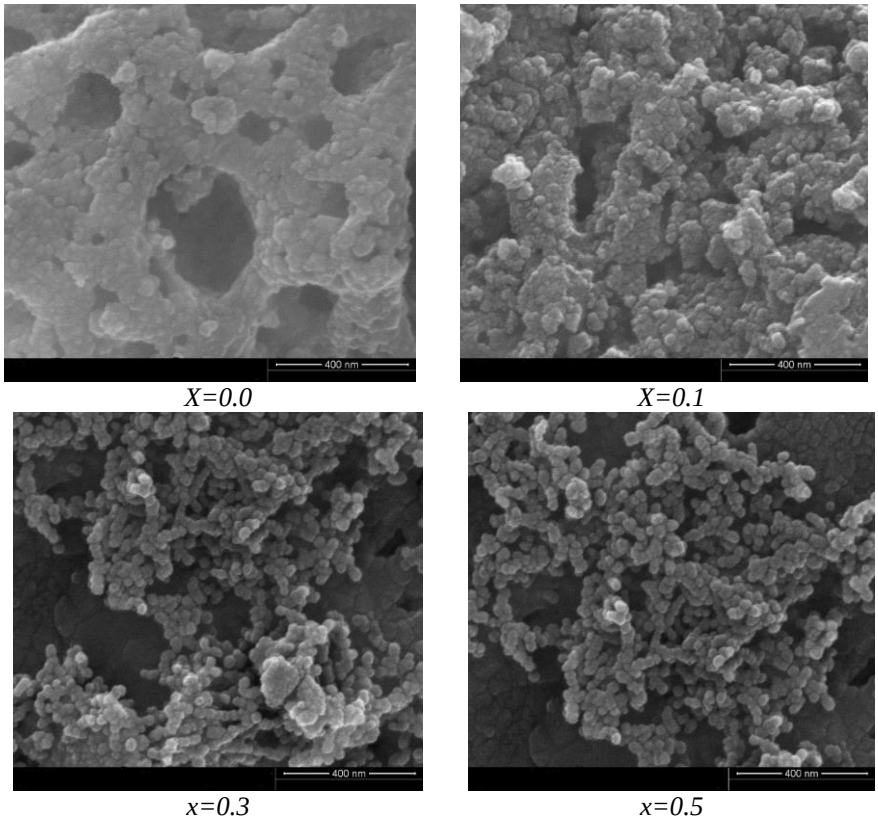

Fig. 5 HR-SEM images of the Mg^{2+} doped Co_3O_4 nanoparticles

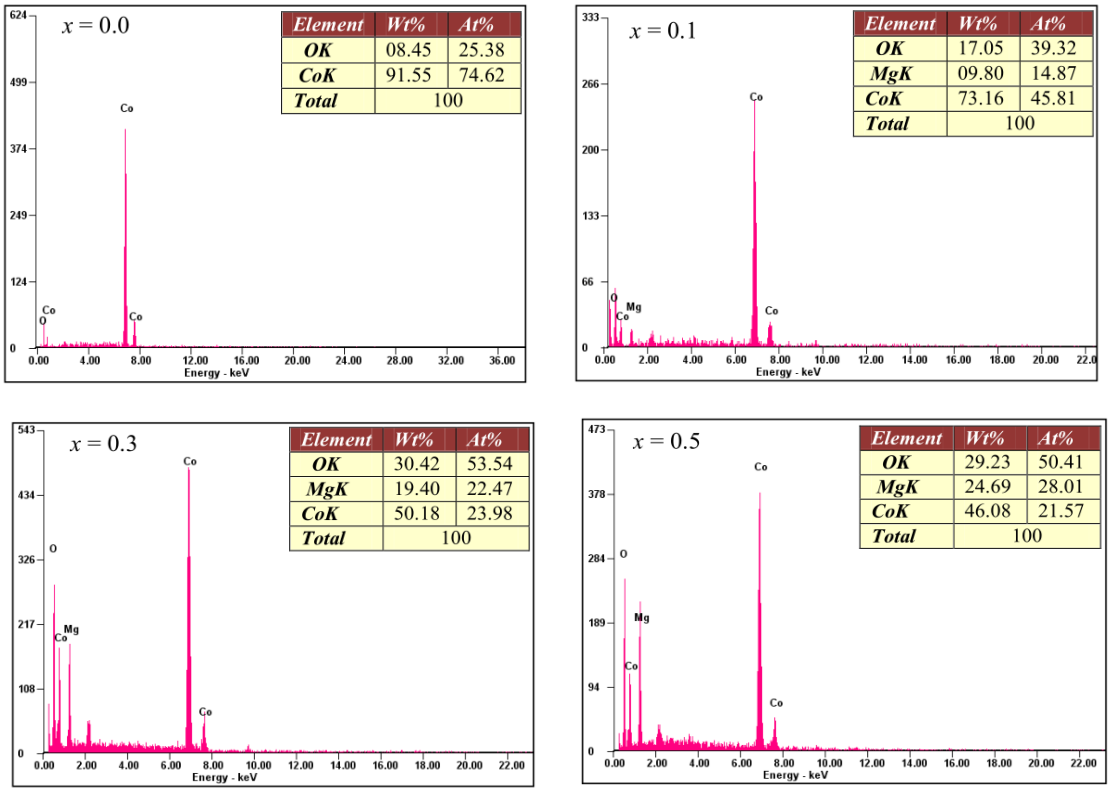

Fig. 6. EDX spectra of the Mg^{2+} doped Co_3O_4 nanoparticles

3.5. Magnetic Studies

The hysteresis curves for Mg^{2+} doped Co_3O_4 NPs showing para and super para magnetic behavior at 0K is shown in Figure 7. Since the cobalt oxide nanoparticles are normal spinel structure, cobalt (III) metal ion is trivalent occupying octahedral site and cobalt (II) metal ion is divalent occupying tetrahedral sites. The saturation magnetization value (M_s) for pure cobalt oxide sample exhibiting paramagnetic behavior is 5.6057 memu g^{-1}. Due to the size effects bulk cobalt oxide shows anti ferromagnetic behavior [17]. The doped sample depicted superparamagnetic behavior and the saturation magnetization values (M_s) are 4.3164, 3.2779 and 2.7238 memu g^{-1} for x = 0.1, 0.3 and 0.5 samples. With increasing Mg^{2+} concentration the coercivity (H_C) and remanent magnetization (M_r) are obtained to be 51.256 to 101.42 Oe and 25.429 to 62.232 μemu g^{-1} correspondingly as given in Table 2. The obtained values are mainly based on the crystallite size and shape of pure and Mg doped cobalt oxide nanoparticles [19, 20].

Table 2. Magnetic properties of Mg^{2+} doped Co_3O_4 nanoparticles.

Mg^{2+}, fraction, *x*	**Coercivity Hc , (Oe)**	**Remanence Mr, (μemu/g)**	**Saturation Magnetization Ms, (memu/g)**
0.0	70.301	48.121	5.6057
0.1	51.256	28.736	4.3164
0.3	101.42	62.232	3.2779
0.5	55.102	25.429	2.7238

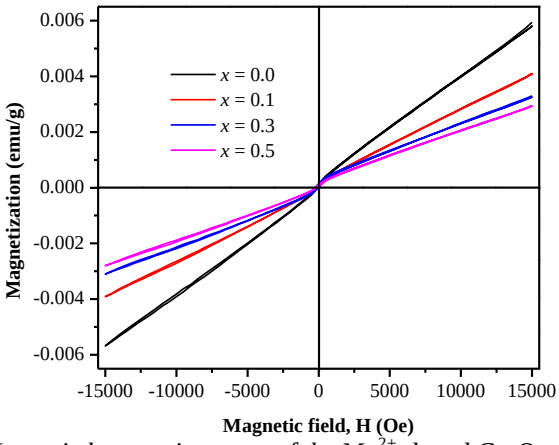

Fig. 7. Magnetic hysteresis curves of the Mg^{2+} doped Co_3O_4 nanoparticles.

4. Conclusion

Utilizing MACM magnesium doped cobalt oxide spinel NPs were prepared. Single phase cubic spinel structure was shown by both pure and Mg doped cobalt oxide NPs (x = 0.1 and 0.2). Due to doping with Mg^{2+} ion a new hexagonal phase was seen. Cubic spinel and hexagonal stretching modes was obtained from Fourier transform infrared spectra at 661 and 573 cm^{-1}. As doping of Mg^{2+} concentration increases the energy gap also increases. SEM images confirmed nanosized crystallized porous grain formation. The

presence of the elements Mg, Co, and O was confirmed through EDX analysis. Para- to super para- magnetic behavior were noticed because of Mg^{2+} doping.

Acknowledgements

The authors express thankful and financial support by the Researchers Supporting Project Number (RSP-2021/354) King Saud University, Riyadh, Saudi Arabia.

References

[1] G. V. M. Williams, T. Prakash, J. Kennedy, Shen V. Chongc, S. Rubanov, J. Magn. Magn. Mater. 460, 229 (2018).
[2] D.S.A. Selvan, M. Keerthi, M. Sundararajan, S. Shobana, B. Lakshmi, V. Veena, A.K. Rahiman, Mater. Chem. Phy., 272, 124903 (2021),
[3] P. Sakthivel, R.J. Ramalingam, D. Pradeepa, S Rathika, C.S. Dash, K. Bhuvaneswari, M. Sundararajan, P.S Subudhi, H.A. Lohedan, J. Nanosci. Nanotech., 21, 5659, (2021).
[4] Ed Lester, Gabriele Aksomaityte, Jun Li, Sara Gomez, Jose Gonzalez-Gonzalez, Martyn Poliakoff, Prog. Cryst. Growth Charact. Mater. 58, 3 (2012).
[5] F. Manteghi, S.H. Kazemi, M. Peyvandipoor, A. Asghari, RSC Adv., 5(93), 1 (2015).
[6] Damian C. Onwudiwe, Murendeni P. Ravele, Elias E. Elemike, Nano-Structures & Nano-Objects 23, 100470 (2020).
[7] N.M. Dang, W.W. Zhao, S. Yusa, H. Noguchi, K. Nakashima, New J. Chem.,39, 4726(2015).
[8] H. BinduDuvuru, S. K. Alla, S. K. Shaw, Sher Singh Meena, Nidhi Gupta, B. B. V. S. Vara Prasad, M. M. Kothawale, M. K. Kumar, N. K. Prasad, Ceram. Int. 45, 16512 (2019).
[9] S. Zhao, J. Guo, W. Li, H. Guo, B. You, Dyes and Pigments, 151, 130 (2018).
[10] L. Qiao, H. Y. Xiao, H. M. Meyer, J. N. Sun, C. M. Rouleau, A. A. Puretzky, D. B. Geohegan, I. N. Ivanov, M. Yoon, W. J. Weber, M. D. Biegalski, J. Mater. Chem. C 1, 4628 (2013).
[11] M. Sundararajan, L. John Kennedy, J. Judith Vijaya, UdayaAruldoss, Spectrochim. Acta Part A Mol. Biomol. Spectrosc. 140, 421 (2015).
[12] Mahmoud Nasrollahzadeh, Babak Jaleh, Ameneh Jabbari, RSC Adv. 4, 36713 (2014).
[13] P.B. Koli, K.H. Kapadnis, U.G. Deshpande, M.R. Patil, J. Nanostr. Chem., 8, 453 (2018).
[14] S.K. Jesudoss, J.J. Vijaya, P.I. Rajan, K. Kaviyarasu, M. Sivachidambaram, L.J. Kennedy, Hamad A. Al-Lohedan, R. Jothiramalingam, M.A. Munusamy, Photochem. Photobiol. Sci., DOI: 10.1039/c7pp00006e.
[15] M. Rashad, Opt Quant Electron., 51, 291 (2019).
[16] M. Sukumar, L. J. Kennedy, J. J. Vijaya, B. Al-Najar, M. Bououdina, New J. Chem. 42, 18128 (2018).
[17] S. Ramachandran, C. S. Dash, A. Tamilselvan, S. Kalpana, M. Sundararajan, J. Nanosci. Nanotechnol. 20(4), 2382 (2020).
[18] V Balachandran, M. Sundararajan, Elixir Vib. Spec. 48, 9663 (2012).
[19] M. Nasrollahzadeh, B. Jaleh and A. Jabbari, RSC Adv., 4, 36713 (2014).
[20] S. Yuvaraj, S. Ramachandran, A. Subramani, A. Thamilselvan, S. Venkatesan, M. Sundararajan, C.S. Dash, J. Supercond. Novel Mag., 33, 1199 (2020).